Electronic Supplementary Material (ESI) for Analyst.

Supplementary Information

Reversible Photo-regulation on the folding/unfolding of Telomere G-quadruplexes with Solid-State Nanopore

Jing Tang[1,2], Ji Wu[1,2], Rui Zhu[2,3], Zhong Wang[1,2], Chuanqi Zhao[4], Peng Tang[1,2], Wanyi Xie[1,2], Deqiang Wang[1,2]*, Liyuan Liang[1,2]*

[1]Chongqing Key Laboratory of Multi-scale Manufacturing Technology, Chongqing Institute of Green and Intelligent Technology, Chinese Academy of Sciences, Chongqing 400714, P. R. China

[2]Chongqing School, University of the Chinese Academy of Science, Chongqing 400714, P. R. China

[3]Chongqing Jiaotong University, Chongqing 400014, P. R. China

[4]Laboratory of Chemical Biology and State Key Laboratory of Rare Earth Resource Utilization, Changchun Institute of Applied Chemistry, Chinese Academy of Sciences, Changchun, Jilin 130022, P. R. China

*Corresponding Authors' e-mail: liangliyuan@cigit.ac.cn, dqwang@cigit.ac.cn

Telomeric sequences used in this work are as follows:

hTelo: 5’-AGGGTTAGGGTTAGGGTTAGGGTT -3’;
c-hTelo: 5’-CCCTAACCCTAACCCTAACCCT-3’;
hTelo-2azof: 5’- AG**X**GG**X**TT AGGGTT AGGGTT AGGGTT -3’
hTelo-2azom: 5’- AGGGTT AGGG**X**TT**X** AGGGTT AGGGTT -3’
hTelo-2azob: 5’- AGGGTT AGGGTT AGGGTT**X** AG**X**GGTT -3’
hTelo-3azo: 5’- AG**X**GGTT AGGGTT**X** AGGGTT AG**X**GGTT -3’
hTelo-3azo-p: 5’- AG**X**GGTT AGGG**X**TTAGGGTT AG**X**GGTT -3’
hTelo-4azo-2p: 5’- AG**X**GGTT AG**X**GGTTAGG**X**GTT AGG**X**GTT -3’
hTelo-4azo-4p: 5’- AG**X**GGTT AGG**X**GTTAG**X**GGTT AGG**X**GTT -3’

In the abbreviation, c: complementary; f: front; m: middle; b: back; p: plane; **X**: azobenzene modification.

hTelo is human telomere sequence without modification; c-hTelo is the complementary sequence of hTelo; hTelo-2azof, hTelo-2azom, hTelo-2azob are two azobenzenes modified on the front, middle, and back of the sequence in which one azobenzene was intercalated in the G4 cavity for hTelo-2azof and hTelo-2azob, and on the loop for hTelo-2azom; hTelo-3azo and hTelo-3azo-p are modified with three azobenzenes, two of them intercalated in the G4 tetrad for hTelo-3azo and one azobenzene coordinated on each quartet plane for hTelo-3azo-p; hTelo-4zao-2p and hTelo-4zao-4p are modified with four azobenzenes, hTelo-4zao-2p contains two azobenzenes diagonally immobilized on each tetrad, while hTelo-4zao-4p holds four azobenzenes on the same G4 tetrad.

Apparatus.

Fluorescence measurements were carried out on a Hitachi F-7000 spectrofluorometer with slit widths of 10 and 10 nm for the excitation and emission, and the fluorescence intensity of all the samples was analyzed via a time base scan (λex = 399 nm, λem = 615 nm). All the measurements were performed with 1 μM of NMM and 0.5 μM of DNA in 1 M CsCl or KCl or LiCl buffer (10 mM Tris, 1mM EDTA, pH 7.4). UV absorbance was recorded on a Metash UV-5500PC UV/Vis spectrophotometer. Polyacrylamide gel electrophoresis (PAGE) (20 %) was carried out in 1 × TBE buffer under a potential of 140 V, 1 μM of DNA samples were melted at 95 ℃ for 5 min. before cooling down to room temperature and incubated in 1 M CsCl buffer for at least 2 h before loading to the gel. After Stains-All staining, gels were scanned. Circular dichroism spectra (CD) were recorded with a JASCO J-810 spectropolarimeter equipped with a temperature-controlled water bath, CD spectra were collected with 10 μM of DNA in 1 M CsCl TE buffer and scanned from 310 to 210 nm in 1 nm increments with an average time of 2 seconds, three scans were accumulated and automatically averaged. The physical size of the nanopore was measured via a transmission electron microscope (Tecnai F20, FEI). Electric pulse breakdown was performed using Keithley 2450 that was controlled by the LabVIEW program to measure the conductivity of the SiNx membrane through the current-voltage (I-V) curves. I-V characteristics and ion current blockade of the samples were measured on a patch-clamp amplifier (Axopatch 200B) sampled at 25 kHz and low-pass Bessel filtered at 5 kHz, which was housed inside a Faraday cage.

Data analysis.

Data analysis was performed on Clampfit and graphed with Origin. All the event spikes were collected at the level of 10-20% of open-pore current which was approximately four times larger than the noise; all dwell time shorter than 0.1 ms or longer than 100 ms and normalized current blockages lower than 0.1 were excluded from the data analysis; all the histograms of the normalized current blockage was divided into 30 bins with a Gaussian fitting and dwell time with an equal bin size of 0.2 ms fitting with exponential decay except special indication.

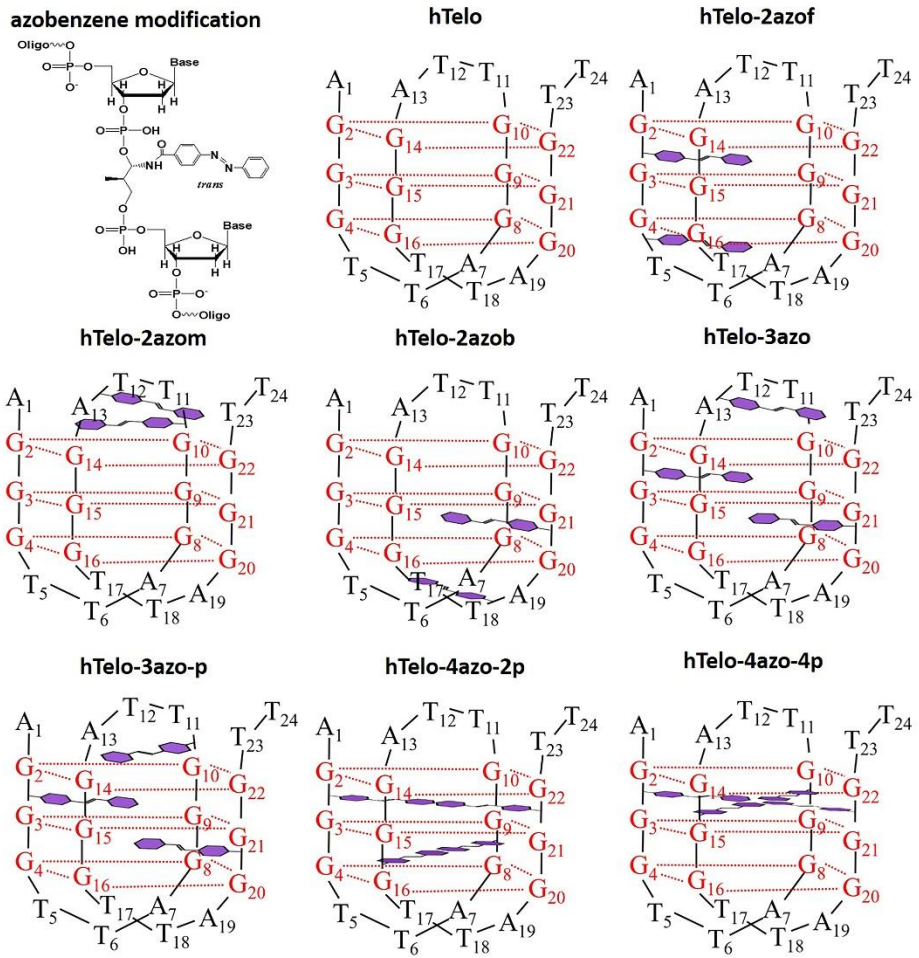

Figure S1. G4 molecular skeletons folded from the human telomere sequences with and without azobenzene modification in 1M CsCl, TE buffer at pH 7.4. In the abbreviation, f: front; m: middle; b: back; p: plane; violet molecule: trans azobenzene isomer. The first chemical structure shows the position of azobenzene on the DNA sequence, the rest represent the G4 skeletons in which the azobenzene were localized.

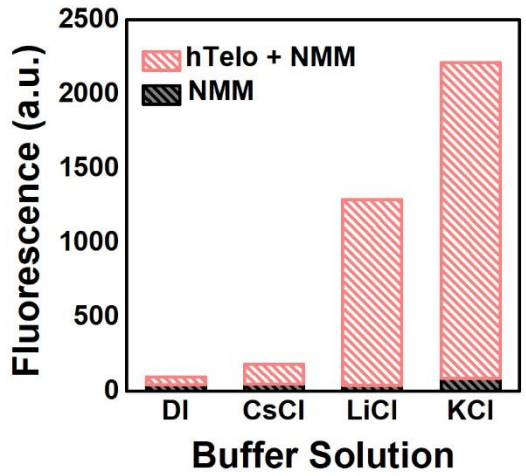

Figure S2. Histograms indicating the fluorescence intensity of 1 µM NMM alone (gray) and the complex of 1 µM NMM and 0.5 µM hTelo (pink) recorded in 1M CsCl, TE buffer at pH 7.4 at λ_{ex} = 399 nm and λ_{em} = 615 nm.

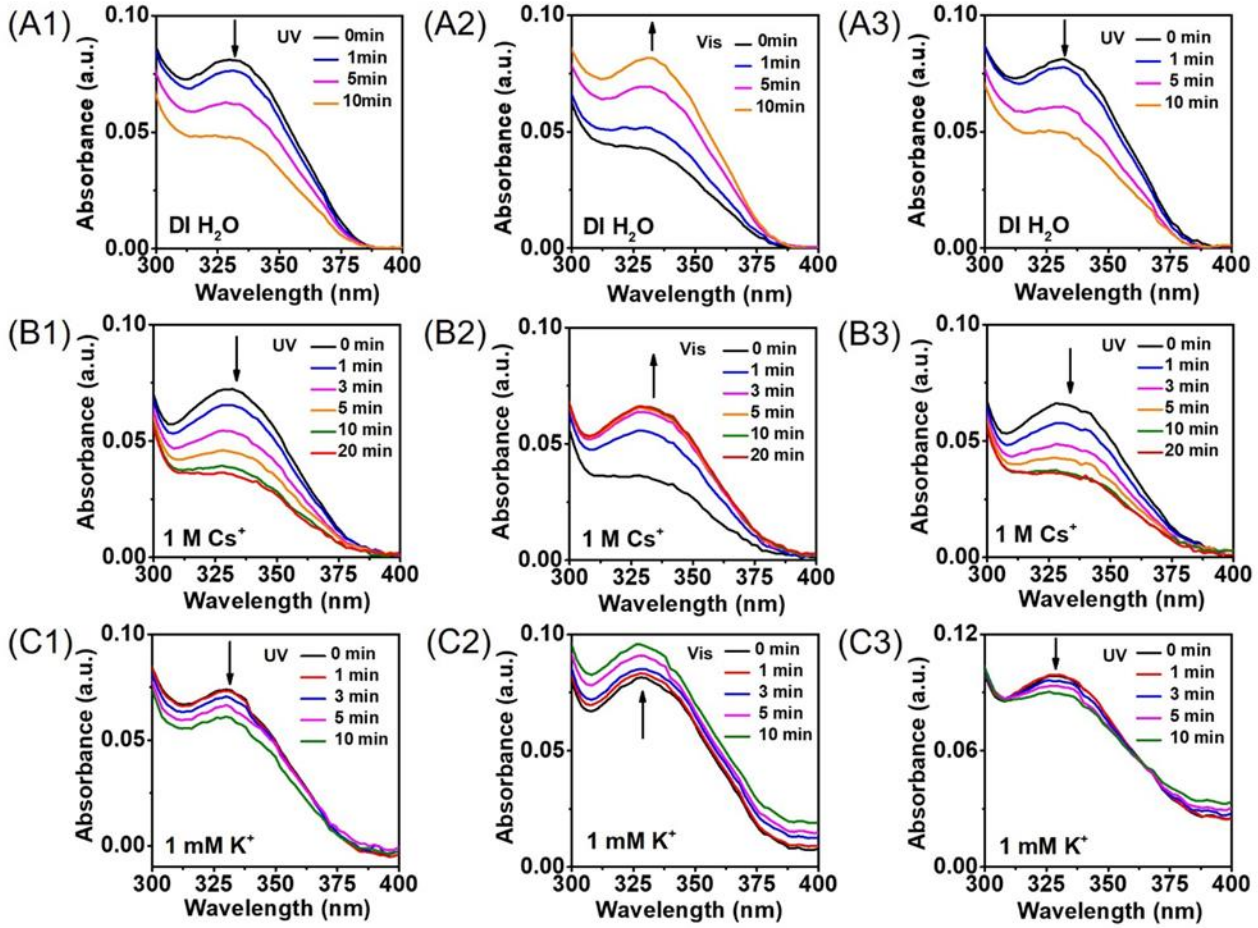

Figure S3. UV spectra of 1 μM hTelo-3azo in (A) DI H_2O, (B) 1 M CsCl, TE buffer at pH 7.4, (C) 1 mM KCl, TE buffer at pH 7.4 under switchable UV-Vis-UV light irradiation from 0 min. to 10 min. or 20 min. as indicated.

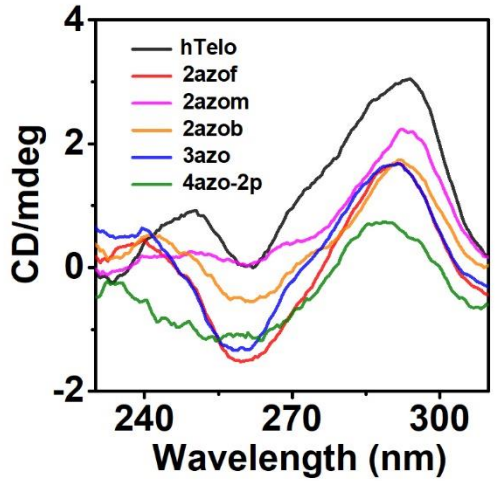

Figure S4. CD spectra of 10 μM of the indicated hTelo G-quadruplexes prepared in 1 M CsCl, TE buffer at pH 7.4 at 22 ℃.

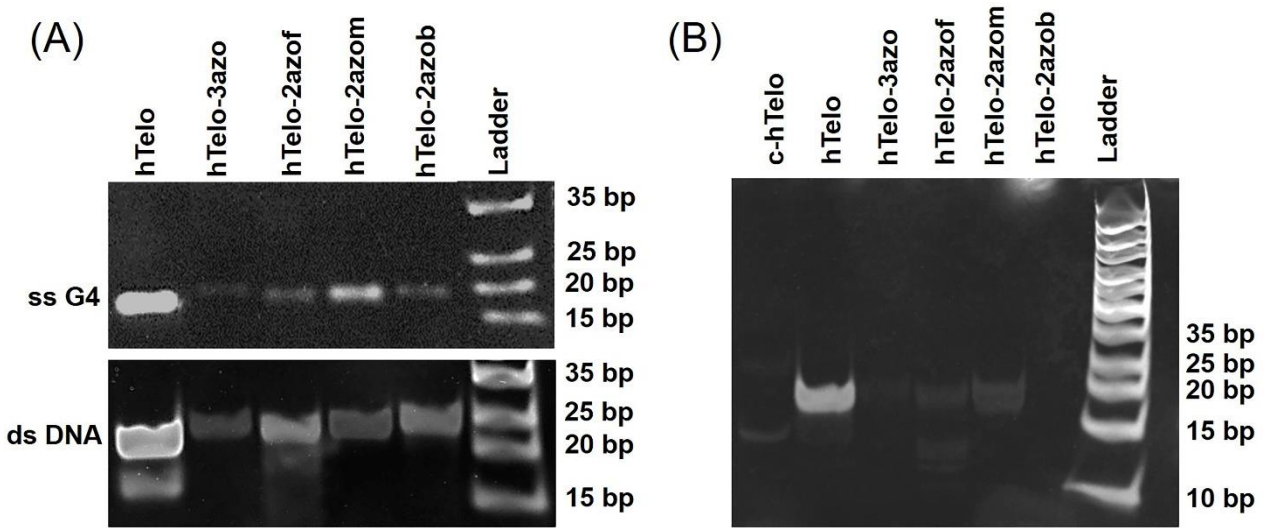

Figure S5. 20% of native PAGE characterization for 1μM of the indicated DNA in 1M electrolyte, TE buffer at pH 7.4, with 1×TBE running buffer under 140 V potential. (A) upper: single-stranded DNA in 1M CsCl; down: double-stranded DNA in 1M CsCl. (B) single-stranded DNA in 1M KCl.

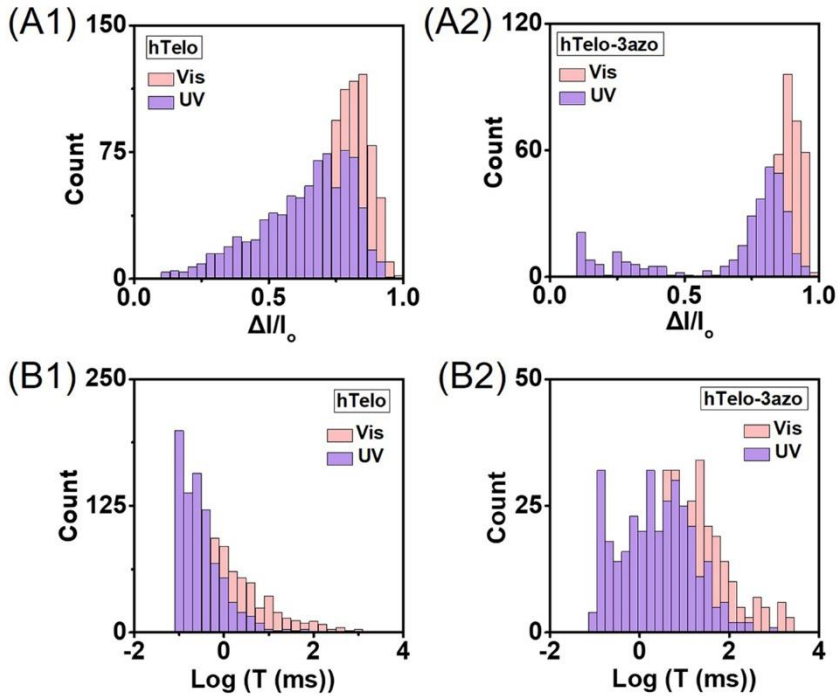

Figure S6. Histograms of the normalized current blockage amplitude (A) and dwell time (B), showing the nanopore translocation properties of 20 nM hTelo with and without azobenzene-modification in 1M CsCl, TE buffer at pH 7.4, under visible (pink) and UV (violet) light irradiation for 2 h, at a voltage of 100 mV. (A1-A2) Histograms of the normalized current amplitude $\Delta I/I_o$ for the indicated DNA that were dividied into 30 bins from 0.1-1. (B1-B2) Histograms of the dwell time for the indicated DNA with a bin size of 0.2 ms.

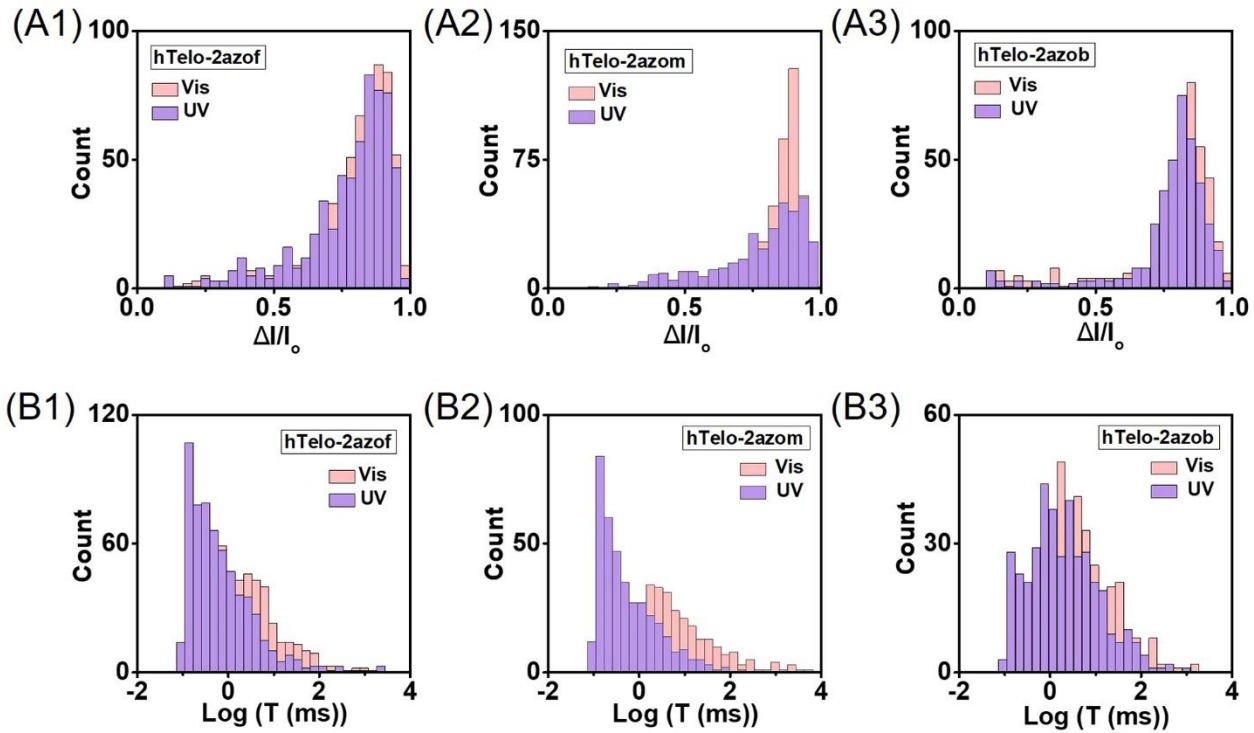

Figure S7. Histograms of the normalized current blockage amplitude (A) and dwell time (B), showing the nanopore translocation properties of 20 nM azobenzene-modified hTelo in 1M CsCl, TE buffer at pH 7.4, under visible (pink) and UV (violet) light irradiation for 2 h, at a voltage of 100 mV. (A1-A3) Histograms of the normalized current amplitude $\Delta I/I_o$ for the indicated DNA that were dividied into 30 bins from 0.1 to 1. (B1-B3) Histograms of the dwell time for the indicated DNA with a bin size of 0.2 ms.

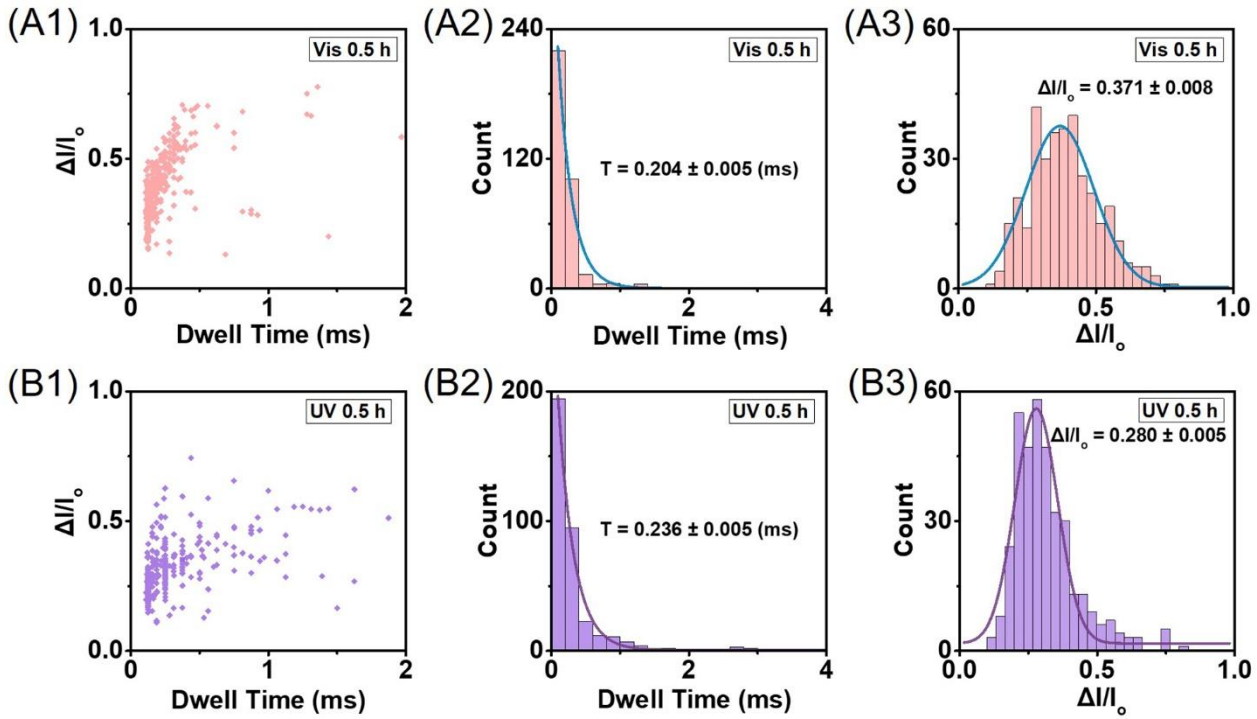

Figure S8**.** Representation of nanopore translocation properties of 20 nM hTelo-3azo in 1M CsCl, TE buffer at pH 7.4, under visible (A) and UV (B) light irradiation for 0.5 h, at a voltage of 100 mV, with a nanopore of 20 nm in thickness and open pore current of 660 pA. (A1-B1) Scatter plots showing event distribution. (A2-B2) Histograms of dwell time with exponential decay fitting curves, all the data were treated with a same bin size of 0.2 ms. (A3-B3) Histograms of the normalized current amplitude with Gaussian fitting curves, all the data of $\Delta I/I_o$ were divided into 30 bins from 0.1 to 1.

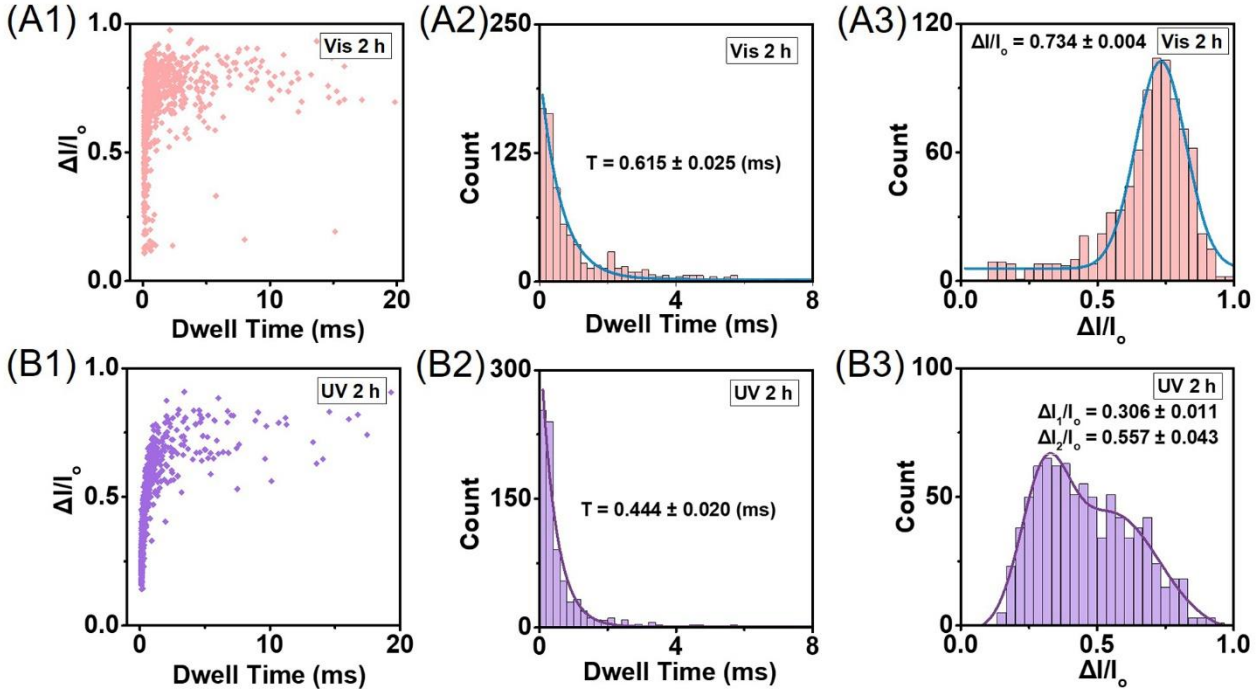

Figure S9. Representation of nanopore translocation properties of 20 nM hTelo-3azo in 1M CsCl, TE buffer at pH 7.4, under visible (A) and UV (B) light irradiation for 2 h, at a voltage of 100 mV, with a nanopore of 20 nm in thickness and open pore current of 570pA. (A1-B1) Scatter plots showing event distribution. (A2-B2) Histograms of dwell time with exponential decay fitting curves, all the data were treated with a same bin size of 0.2 ms. (A3-B3) Histograms of the normalized current amplitude with Gaussian fitting curves, all the data of $\Delta I/I_o$ were divided into 30 bins from 0.1 to 1.

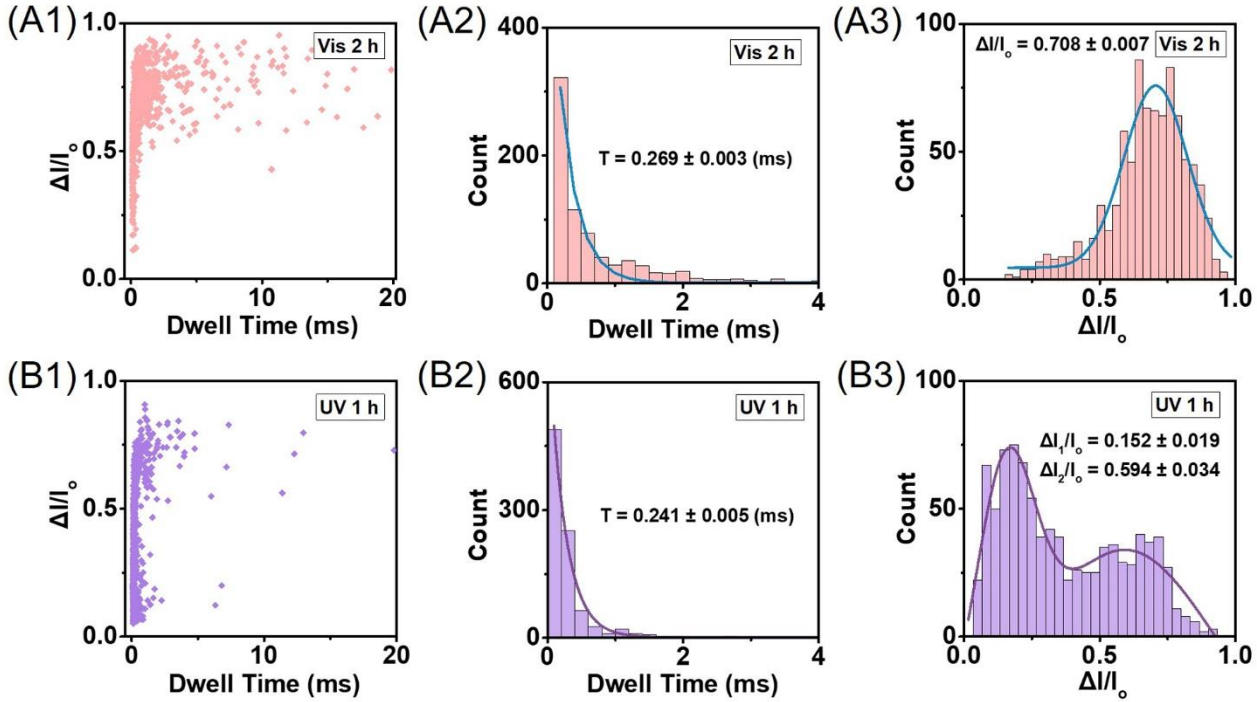

Figure S10. Representation of nanopore translocation properties of 20 nM hTelo-3azo-p in 1M CsCl, TE buffer at pH 7.4, under visible light irradiation for 2 h (A) and UV light irradiation for 1h (B) , at a voltage of 100 mV, with a nanopore of 20 nm in thickness and open pore current of 590 pA. (A1-B1) Scatter plots showing event distribution. (A2-B2) Histograms of dwell time with exponential decay fitting curves, all the data were treated with a same bin size of 0.2 ms. (A3-B3) Histograms of the normalized current amplitude with Gaussian fitting curves, all the data of $\Delta I/I_o$ were divided into 30 bins from 0.1 to 1.

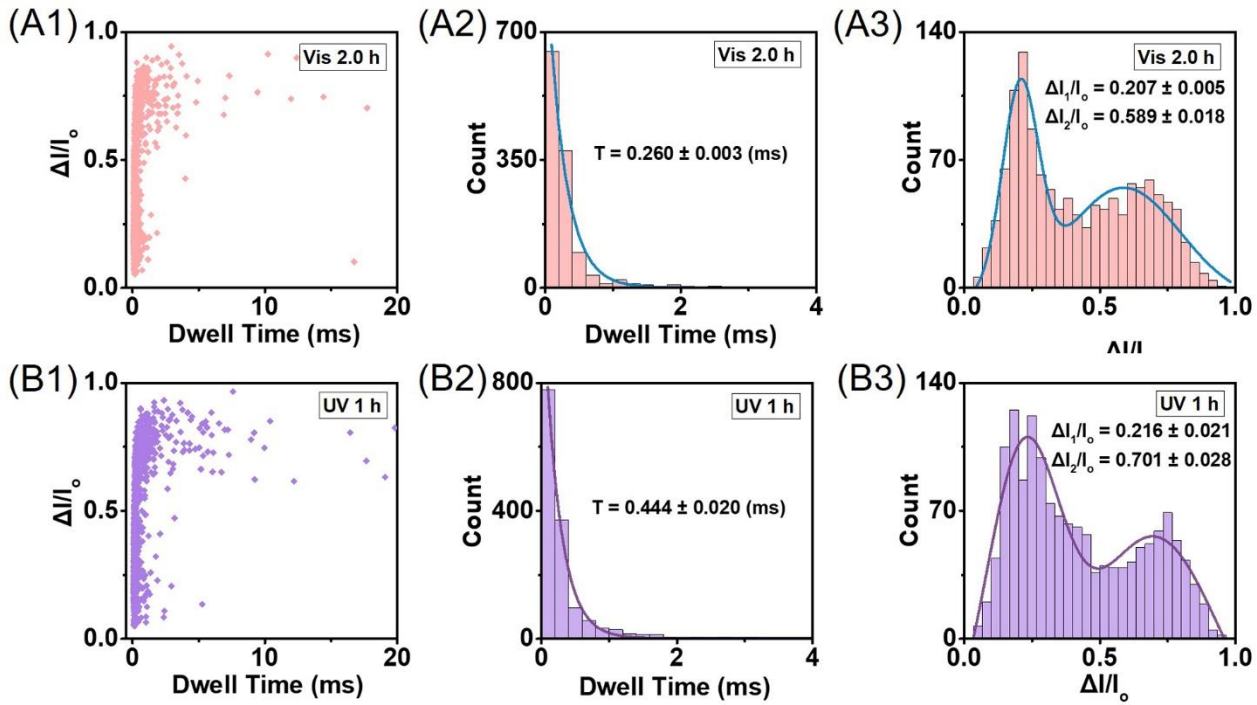

Figure S11. Representation of nanopore translocation properties of 20 nM hTelo-4azo-2p in 1M CsCl, TE buffer at pH 7.4, under visible light irradiation for 2 h (A) and UV light irradiation for 1h (B) , at a voltage of 100 mV, with a nanopore of 20 nm in thickness and open pore current of 590 pA. (A1-B1) Scatter plots showing event distribution. (A2-B2) Histograms of dwell time with exponential decay fitting curves, all the data were treated with a same bin size of 0.2 ms. (A3-B3) Histograms of the normalized current amplitude with Gaussian fitting curves, all the data of I/I_o were divided into 30 bins from 0.1 to 1.

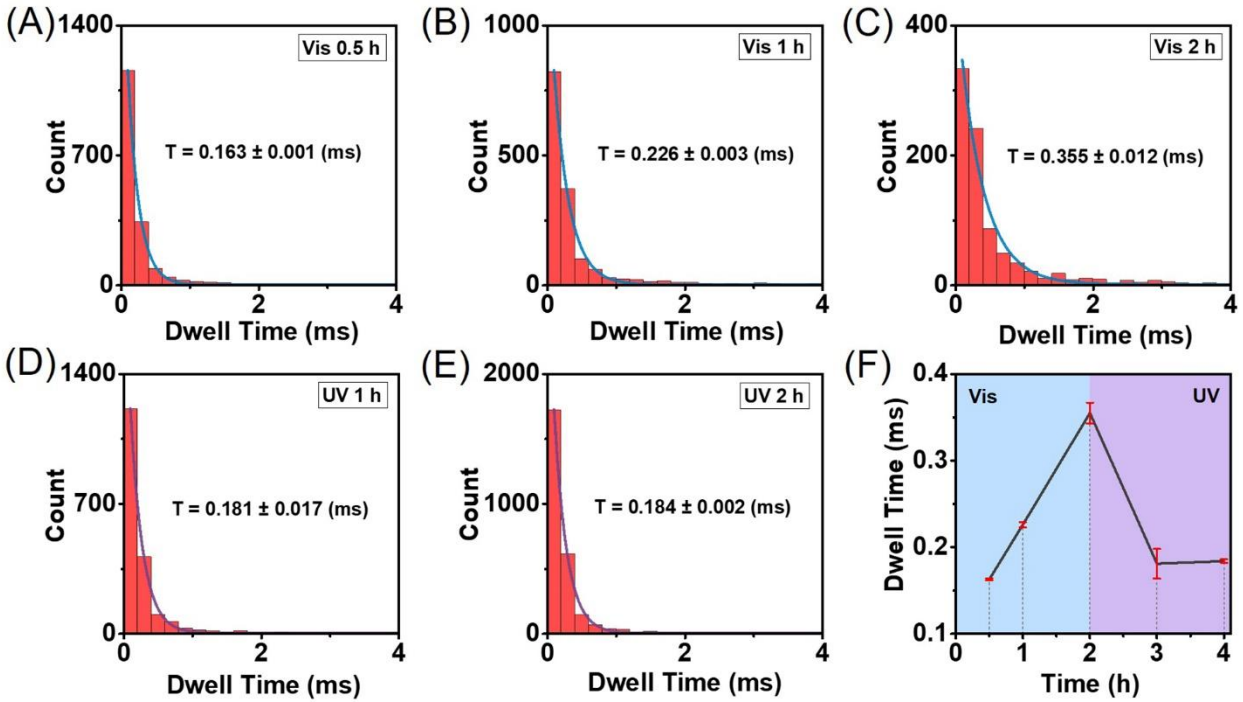

Figure S12. Histograms and line graph of the dwell time showing the translocation properties with 20 nM hTelo-3azo-p in 1M CsCl, TE buffer at pH 7.4 under 100 mV, upon visible light irradiation for 0.5 h (A), 1 h (B) and 2 h (C)； and UV light irradiation for 1 h (D) and 2 h (E). (F) Line graph of the dwell time as a function of light exposure for different time, blue region represents the visible light irradiation and violet region represents UV light treatment. Line graph was produced from the exponential decay fitting values of the histograms in A-E with a bin size of 0.2 ms, the data represent the means ± SD of the fitting values.

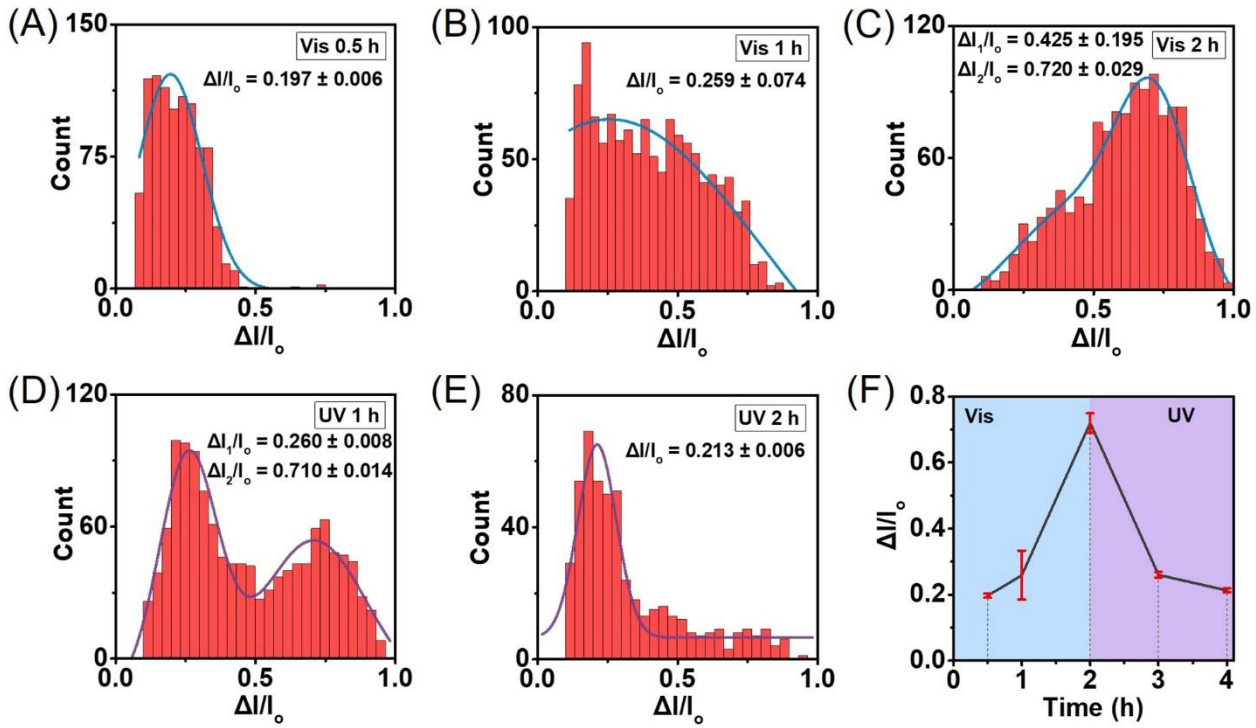

Figure S13. Histograms and line graph of normalized current blockage amplitude showing the translocation properties with 20 nM hTelo-4azo-4p in 1M CsCl, TE buffer at pH 7.4 under 100 mV, upon visible light irradiation for 0.5 h (A), 1 h (B) and 2 h (C)； and UV light irradiation for 1 h (D) and 2 h (E). (F) Line graph of the normalized block amplitude $\Delta I/I_o$ as a function of light exposure for different different time, blue region represents the visible light irradiation and violet region represents UV light treatment. Line graph was produced from the Gaussian fitting values of the histograms of $\Delta I/I_o$ in A-E that were divided into 30 bins, the data represent the means ± SD of the fitting values.

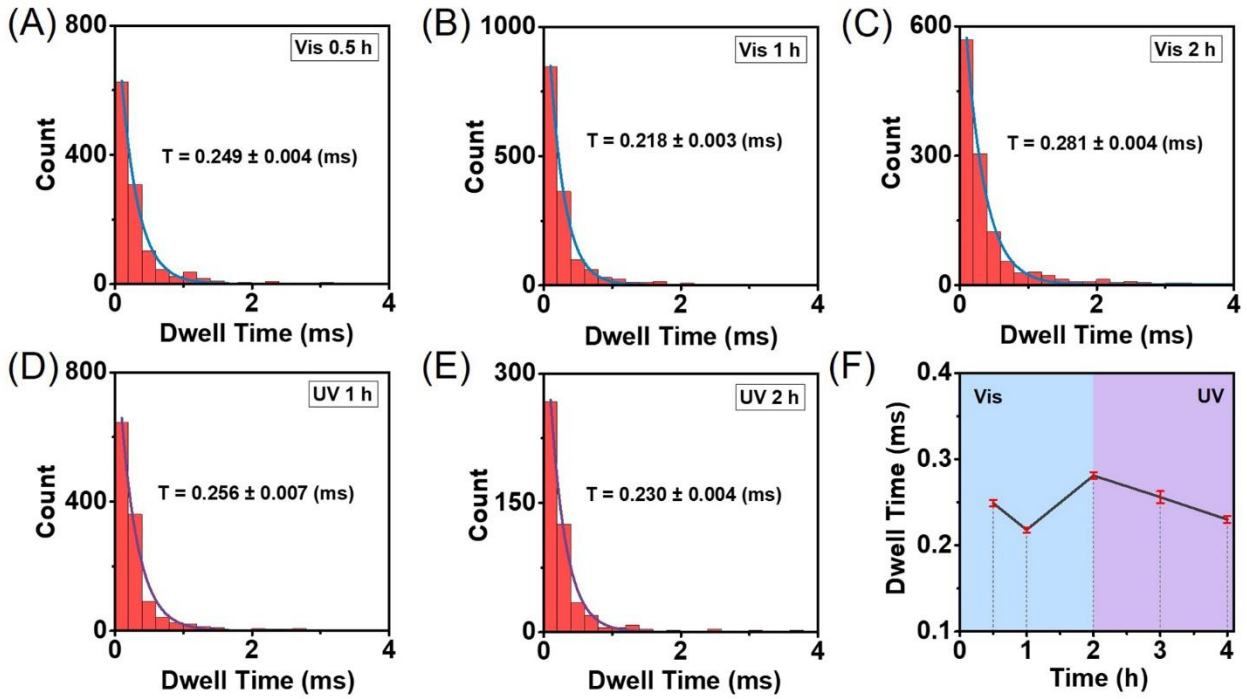

Figure S14. Histograms and line graph of the dwell time showing the translocation properties with 20 nM hTelo-4azo-4p in 1M CsCl, TE buffer at pH 7.4 under 100 mV, upon visible light irradiation for 0.5 h (A), 1 h (B) and 2 h (C)； and UV light irradiation for 1 h (D) and 2 h (E). (F) Line graph of the dwell time as a function of light exposure for different time, blue region represents the visible light irradiation and violet region represents UV light treatment. Line graph was produced from the exponential decay fitting values of the histograms in A-E with a bin size of 0.2 ms, the data represent the means ± SD of the fitting values.

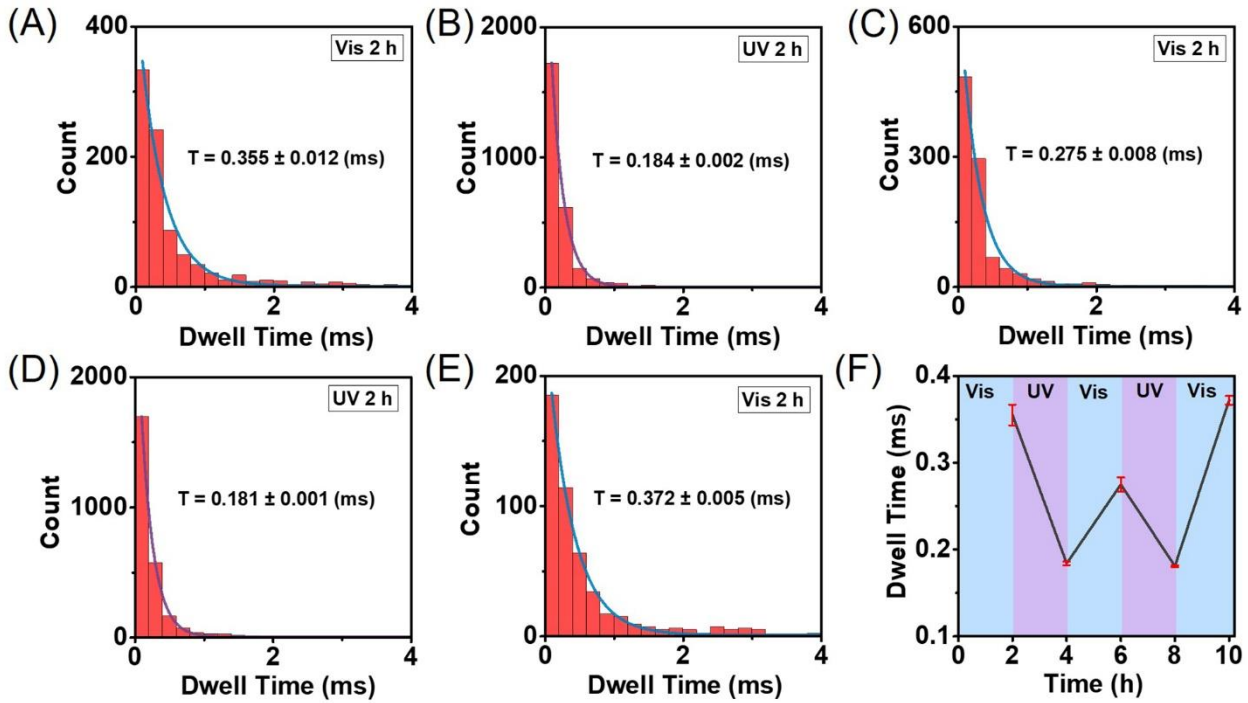

Figure S15. Histograms and line graph of the dwell time of 20 nM hTelo-3azo-p in 1M CsCl, TE buffer at pH 7.4 under 100 mV, showing the revisibility of the G4 folding/unfolding upon Vis/UV light switch. (A) Vis 2 h; (B) UV 2 h; (C) Vis 2 h; (D) UV 2 h; (E) Vis 2 h. (F) Line graph of the dwell time as a function of switchable Vis/UV exposure for 2 h, blue region represents the visible light irradiation and violet region represents UV light treatment. Line graph was produced from the exponential decay fitting values of the histograms in A-E with a bin size of 0.2 ms, the data represent the means ± SD of the fitting values.

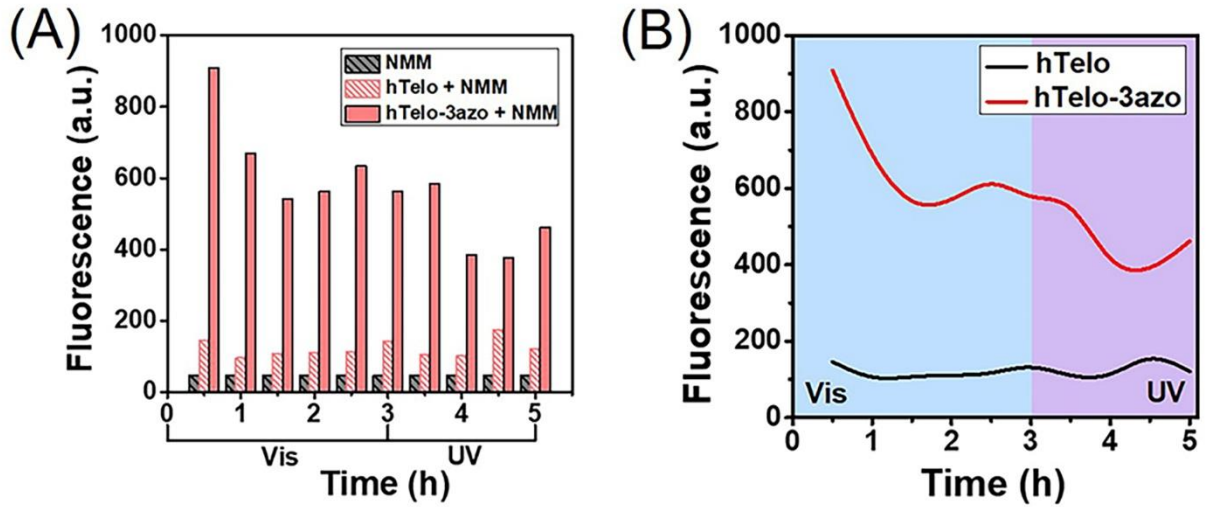

Figure S16. Fluorescence characterization. (A) Histograms indicating the fluorescence intensity of 1 μM NMM alone (gray), the complex of 1 μM NMM and 0.5 μM hTelo (pink), and the complex of 1 μM NMM and 0.5 μM hTelo-3azo (red) recorded in 1M CsCl, TE buffer at pH 7.4, recorded at λ_{ex} = 399 nm. (B) Line graphs of the fluorescence intensity of hTelo-3azo (black) and hTelo (red) at λ_{em} = 615 nm under switchable Vis/UV exposure for different time. Blue region represents the visible light irradiation and violet region represents UV light treatment.